



# Topological Optimal Material Design of Structures with Moved and Regularized Heaviside Function

Dongkyu Lee<sup>1</sup> · Soomi Shin<sup>2</sup>

Received: 10 September 2014 / Accepted: 20 December 2017 / Published online: 2 August 2018  
© Shiraz University 2018

## Abstract

This study presents a new regularized penalty form to carry out material topology optimization of structures. In general, the regularization form of typical SIMP has been used to reduce material discontinuity of densities which describe boundaries of finite elements and finally provide numerical stability in sensitivity analysis of optimization procedures and the problem of 0–1 formulation. However, optimal solutions of the regularized SIMP depend on penalty parameters such as typical SIMP, since penalty relation of Young's modulus and density of regularized SIMP is similar to that of typical SIMP in spite of regularization. In this paper, the penalty relationship between Young's modulus and material density of typical SIMP becomes extended by multiplying it with a moved and regularized form of a material indication function, i.e., Heaviside function. The new penalization method does not depend on filter methods for free-checkerboards; therefore, computational savings can be obtained. Numerical examples demonstrate that the incorporation of moved and regularized Heaviside function in the SIMP leads to convergent solutions with clear boundaries between materials and no materials and without checkerboard patterns.

**Keywords** Structural topology optimization · SIMP · 0–1 formulation · Material indication function · Moved and regularized Heaviside function

## 1 Introduction

Topology optimization for continuum structures has reached a level of maturity whereby it is being implemented in many industrial problems such as civil and architectural structures as well as airplanes, ships, and autos. Topology optimization is a rapidly expanding field of structural mechanics and can yield much greater savings than mere size or shape optimization. Numerical process of topology optimization is usually done by meshing design domains and determining material contents, i.e., densities, of each finite element. Design variables are connected one-to-one to the finite elements and thus the number of design variables is proportional to that of finite elements and

consequently leads to many design variables for the optimization. Note that the number of elements must be relatively high due to the fact that grids should be sufficiently refined to represent appropriate geometrical features and proper response fields. However, refined meshes give rise to many computation burdens.

Using topology optimization, limited problems of shape optimization (Zienkiewicz and Campbell 1973; Pahlevani and Ebrahimi 2013) depending on initial topology of structure are avoided. Topology optimization is itself different from shape optimization based on boundary variations in the fact that no pre-information of initial topology and shape of designs is supplied to the optimization processes and both optimal shape and topology can be yielded as optimal solutions.

Topology optimization problem can be regarded as a material distribution problem. It is well known that it may be a generally ill-posed problem, i.e., no solutions exist. Cheng and Olhoff (1981) suggested that the main difficulty in topology optimization is an ill-posed problem so that its 0–1 formulation is mesh dependent; therefore, this design

✉ Soomi Shin  
shinsumi82@pusan.ac.kr

<sup>1</sup> Department of Architectural Engineering, Sejong University, Seoul 143-747, Korea

<sup>2</sup> Research Institute of Industrial Technology, Pusan National University, Busan 609-735, Korea

is not optimal since it can be improved by further mesh-refinement. In this context, Sigmund and Petersson (1998) and Diaz and Sigmund (1995) demonstrated that numerical instabilities, i.e., singularities of solutions related with mesh-dependence, checkerboards and local minima occur in topology optimization problem.

In order to overcome the above problems, an important development in topology optimization is a homogenization method to constitute well-posed problem as devised by Bendsøe and Kikuchi, in which a material model with micro-scale voids is introduced and the topology optimization problem is defined by searching the optimal porosity as introduced by Bendsøe (1989), Bendsøe and Haber (1993), Fujii et al. (2001). However, the homogenization method may not yield manufacturable optimal structures, since it often produces designs with infinitesimal pores in the materials.

Additionally, many attempts of the homogenization method have been investigated, for example, the method for continuous variables to be replaced by integers and to be forced into discrete values of penalization, i.e., “Solid Isotropic Material with Penalization” (SIMP) approach (Diaz and Bendsøe 1992; Bendsøe and Sigmund 1999; Sigmund 2001; Bourdin 2001). In practical engineering’s point of views, SIMP approach comes over the manufacture problem of solutions which occurs in typical homogenization method and it has been very often utilized in ranges of topology optimization problem due to numerical simplicity of the application. However, weakness of physical description about the penalization relation of design variables and Young’s modulus remain as the major difficulties for realistic requirements.

The penalization is controlled by penalty parameter and its value must be appropriately determined by structural problem, since it decides the quality of optimal solution. It is commonly known that the value over 3.0 is proper. In this study, note that the penalized form of typical SIMP approach originally includes a material indication concept: i.e., Heaviside function, which defines the signals of 0–1 formulation. For the purpose of numerical stability to calculate sensitivity analysis and produce non-singular solutions, Heaviside function must be regularized in topology optimization problem. Here, it is assumed that both penalty form and regularization form of Heaviside function exist in optimization problem. In addition, because of restriction of design variable values  $[0, 1]$ , the regularized Heaviside function is moved toward  $x$  axial coordinate and becomes a new function which has domain  $[0, 1]$ . The function is named as “Moved and Regularized Heaviside Function”, i.e., MRHF.

The penalization form which is multiplied with MRHF makes more improved artificial materials with small penalty parameter value compared with typical SIMP, since a

generally too large value of the parameter may give rise to numerical singularity. This coupled value of element density and regularization is then constantly assigned onto each finite element, and the element-based topology optimization produces the final distribution contour of element density without mesh-dependence and checkerboard patterns. These benefits are realized without any additional filter method in typical SIMP approach.

Regularization of the discontinuity function of material indicator in topology optimization is not a new idea. Belytschko et al. (2003) and Guest et al. (2004) reported success using the regularized Heaviside function to implicitly describe the topology and archive numerical stability of optimization. The approach presented here differs in the fact that the moved and regularized Heaviside function is additionally used as a partial term of total penalization in the SIMP approach and the penalization including MRMF is regarded as an artificial and new material model.

The layout of the present study is as follows. In Sect. 2, the goal and intuitive idea of this present method is discussed and thus the typical SIMP approach and the moved and regularized Heaviside function are introduced. The well-known material topology optimization problem in which the proposed penalization becomes implemented is formulated in Sect. 3. In Sect. 4, an analytical sensitivity method with a variational approach is described to utilize an adjoint method of Lagrangian multiplier as introduced by Haug et al. (1986) and Haftka and Guerdal (1992). In Sect. 5, the numerical efficiency of the proposed SIMP approach using MRHF is verified through numerical examples and compared with that of typical SIMP and filter method. Finally, conclusions are given in Sect. 6.

## 2 Goal and Intuitive Idea

### 2.1 SIMP Approach

In continuous formulations of topology optimization problem, the design is given by a continuous scalar function  $\Phi$  from the fixed design domain  $\Omega_x \subseteq \mathbb{R}^n$  ( $n = 2$  or  $3$ ) to the allowed material density  $0 \leq \Phi \leq 1$ . After discretization process of the continuous design domain, the material density  $\Phi_i$  is constantly assigned onto each finite element and is defined by applying a penalty contour to the design variable field, i.e., as in the so-called “power law approach” or SIMP approach (Bendsøe and Kikuchi 1988).

According to the approach, the material density distribution has an effect on the element stiffness. Thus, the element stiffness–density relationship may be expressed in terms related to Young’s modulus  $E$ , i.e.,  $E_i$  is assigned by the updated element density  $\Phi_i$  and is defined as

$$E_i(\Phi_i) = E_0 \left( \frac{\Phi_i}{\Phi_0} \right)^k ; i = 1 \dots n, n$$

= total number of element (1)

where  $E_0$  and  $\Phi_0$  are, respectively, nominal values of Young’s modulus and material density. The penalty parameter  $k \geq 1$  penalizes intermediate material densities as shown in Fig. 1 and is incremented throughout the optimization process.

For example, and without loss of generality, an isotropic material model with a plane stress (such as a wall structure) is used here, so that

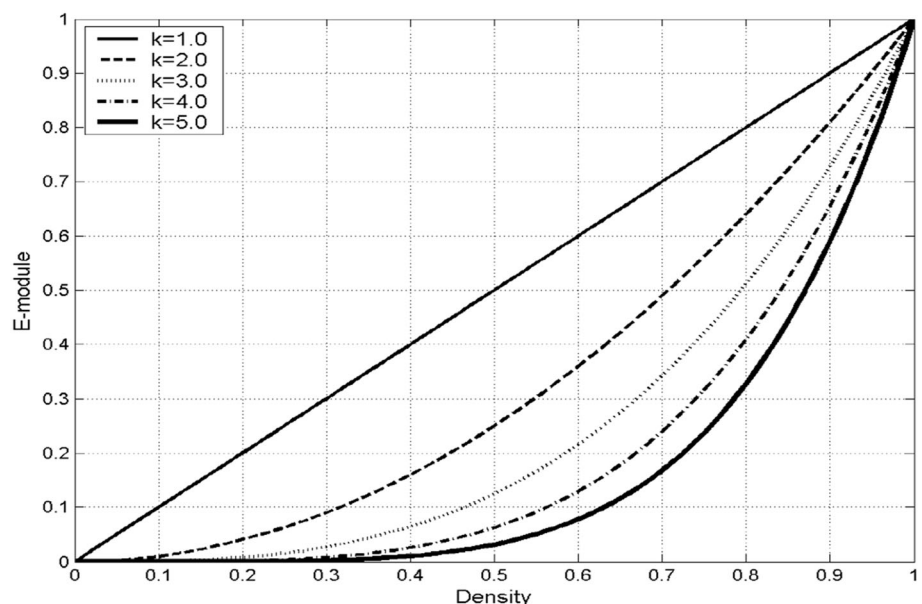
$$C_i = \frac{E_i(\Phi_i)}{1 - \nu^2} \begin{bmatrix} 1 & \nu & 0 \\ \nu & 1 & 0 \\ 0 & 0 & \frac{1 - \nu}{2} \end{bmatrix}$$
 (2)

where  $C_i$  is a material tensor of each finite element  $i$  and includes the updated term of Young’s modulus  $E_i$  defined by the updated element density  $\Phi_i$ .  $\nu$  is Poisson’s ratio. Here, the minimal strain energy on a linear elastic structure is utilized as an objective function of topology optimization problem and is defined as

$$\text{Minimize } f = \frac{1}{2} \int_{\Omega_x} \varepsilon^T C_i \varepsilon \, d\Omega_x$$
 (3)

where, the material tensor  $C_i$  depending on updated element densities automatically includes an indication function as signals of void phase (0)—solid phase (1) in SIMP approach. Therefore, the signals need not be defined in typical SIMP approach. However, note that it is assumed in this study that an explicit indication function, i.e., Heaviside function, is applied to design domain. The objective function with Heaviside function is again defined as:

**Fig. 1** Penalty relationship between Young’s modulus and element density with various penalty parameter  $k$



$$\text{Minimize } f = \frac{1}{2} \int_{\Omega_x} H(\Phi_i) \varepsilon^T C_i \varepsilon \, d\Omega_x$$
 (4)

According to fixed ranges of element material density  $0 \leq \Phi_i \leq 1$ , Heaviside function is defined as

$$H(\Phi_i) = \begin{cases} 0 & \text{if } \Phi_i < 0 \\ 1/2 & \text{if } \Phi_i = 0 \\ 1 & \text{if } \Phi_i > 0 \end{cases}$$
 (5)

and Heaviside function with 0–1 formulation and its expression in the design domain are shown in Fig. 2.

### 2.2 Moved and Regularized Heaviside Function

When executing topology optimization process, large jumps in density  $\Phi_i$  across the interface (for example, at the boundary) may cause numerical instabilities such as singularities of solutions. Moreover, the objective function with discontinuous Heaviside function would make it unworkable to obtain its sensitivity, since the derivative of Heaviside function is Dirac delta function. Special care must therefore be taken here. In order to prevent these numerical difficulties, it is common to introduce regularization of discontinuous Heaviside function introduced by Belytschko et al. (2003). As shown in Fig. 3, since domains of the regularized Heaviside function do not identify with ranges of design variable [0, 1], the continuous function must be transferred toward  $x$  axial coordinate with the magnitude of 0.5. The moved and regularized Heaviside function (Lee and Shin 2015) is illustrated in Fig. 3. Here,  $\chi$  is an interface thickness and generally is 0.5.

**Fig. 2** Heaviside function with 0–1 formulation and its expression in design domain **a** Heaviside function **b** 2-D design domain with solids and voids **c** 3-D design domain with solids and voids

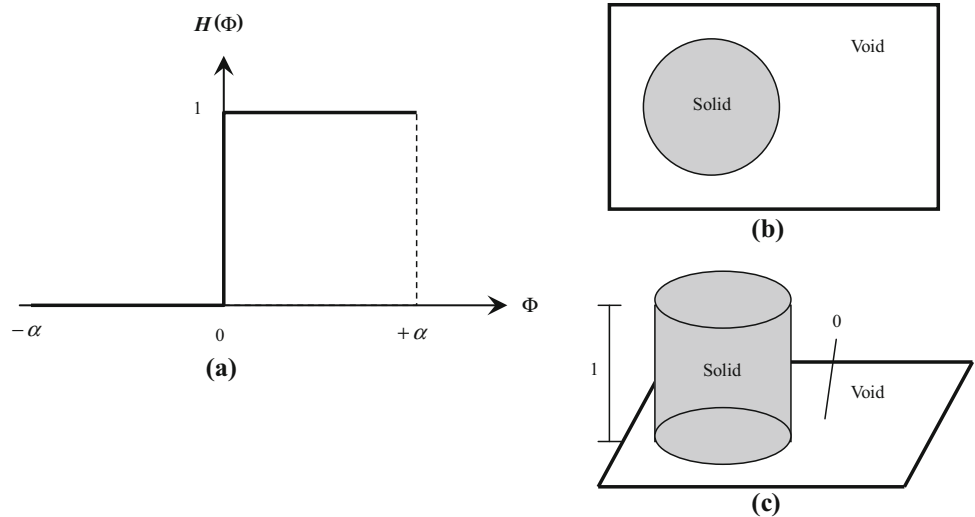
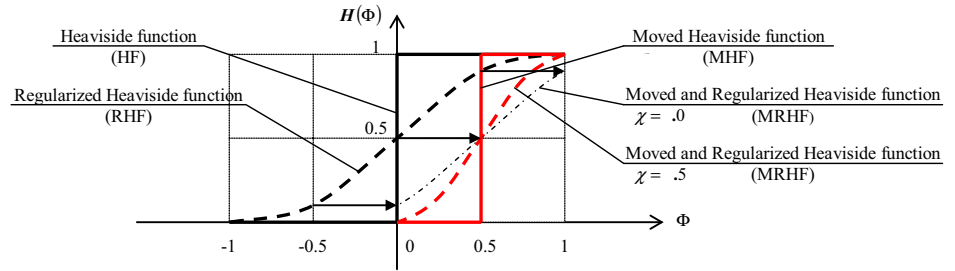


**Fig. 3** Moved and regularized heaviside function (MRHF)



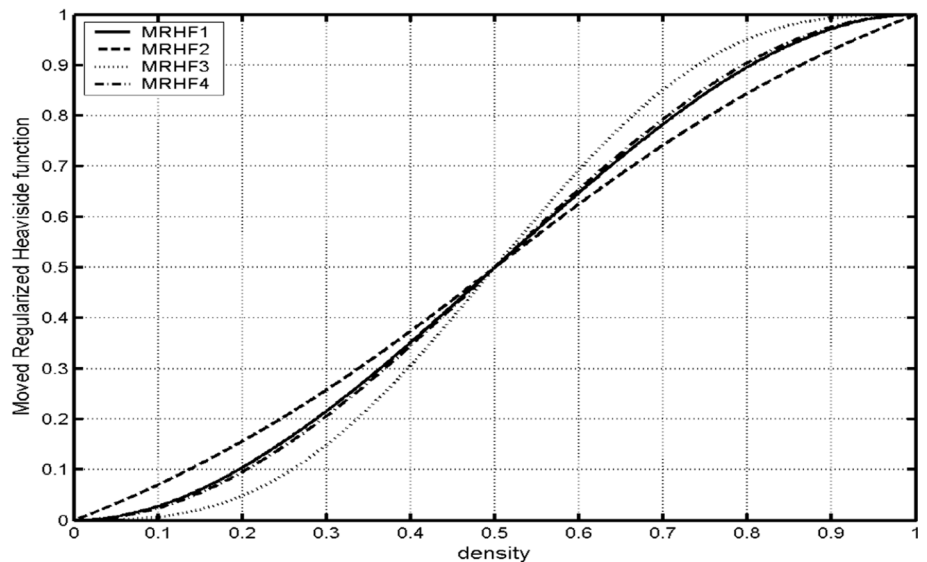
Various types of MRHF can be applied to regularize Heaviside function and they are formulated as follows and shown in Fig. 4.

$$MRHF_1(\Phi) = \frac{3}{4} \left[ \frac{\Phi - 0.5}{\chi} - \frac{1}{3} \left( \frac{\Phi - 0.5}{\chi} \right)^3 \right] + \frac{1}{2} \quad (6)$$

$$MRHF_2(\Phi) = \frac{1}{2} + \frac{2}{\pi} \arctan \left( \frac{\Phi - 0.5}{\chi} \right) \quad (7)$$

$$MRHF_3(\Phi) = \frac{1}{2} \left[ 1 + \frac{\Phi - 0.5}{\chi} + \frac{1}{\pi} \sin \left( \frac{\pi(\Phi - 0.5)}{\chi} \right) \right] \quad (8)$$

**Fig. 4** Moved and regularized Heaviside function of four types in  $\chi = 0.5$



$$\text{MRHF}_4(\Phi) = \frac{1}{2} \left[ 1 + \sin\left(\frac{\pi(\Phi - 0.5)}{2\chi}\right) \right] \quad (9)$$

Equation (4) can be expressed as a new objective function including MRHF and it is rewritten as

$$\text{Minimize } \bar{f} = \frac{1}{2} \int_{\Omega_x} \text{MRHF}(\Phi_i) \varepsilon^T C_i \varepsilon \, d\Omega_x \quad (10)$$

### 2.3 Penalization Effect of Moved and Regularized Heaviside Function

From Eq. (10), it can be seen that the penalty form of typical SIMP is multiplied with a moved regularization of Heaviside function. Applying the same penalty parameter  $k = 3.0$ , gradient of penalty function (PF) with MRHF is greater than that of original penalty function as shown in Fig. 5a. It seems that the gradient effect is  $\text{MRHF3} > \text{MRHF4} > \text{MRHF1} > \text{MRHF2}$  from Fig. 4. Gradient of Heaviside function is defined as Dirac delta function and Fig. 5b illustrates RDDF and MRDDF, i.e., Dirac delta functions of RHF and MRHF, respectively.

The key effect of SIMP approach using MRHF is that it can be produced due to the great gradient of penalization relation as follows: (1) Obvious material distribution contours without gray scales (2) Free-checkerboard patterns. Therefore, numerical computation of optimization can be saved because it is not necessary to use filter method (Sigmund 2001) to remove checkerboard pattern. The origin of this pattern is unclear, but it will be shown in Sect. 5.4 that it is a purely numerical phenomenon and does not have any physical importance.

### 3 Topology Optimization Problem: Displacement Approach as a Minimization of Total Potential Energy

In this paper, a linear elastostatic problem is considered to describe the problem of the structural topology optimization. Let  $\Omega_x \subseteq \mathbb{R}^n (n = 2 \text{ or } 3)$  be a design domain occupied by a linear isotropic elastic structure. The boundary condition of  $\Omega_x$  is composed of three parts, i.e.,  $\Gamma = \partial\Omega_x = \Gamma_x \cup \Gamma_t \cup \Gamma_u$  with the Neumann boundary condition on  $\Gamma_t$ ; the Dirichlet condition on  $\Gamma_u$ ; and the traction free, boundary segment on  $\Gamma_x$ . Respectively, they are written as:

$$\bar{t} = t_0 \text{ on } \Gamma_t \quad (11)$$

$$\bar{u} = u_0 \text{ on } \Gamma_u \quad (12)$$

where  $t_0$  and  $u_0$  are given traction forces (or surface loads) and displacement fields. The field condition of  $\Omega_x$  consists of a balanced, constitutive and kinematic condition, and they are expressed as:

$$\text{div } \sigma + \bar{b} = 0 \quad (13)$$

$$\sigma = C\varepsilon \quad (14)$$

$$\varepsilon = Lu \quad (15)$$

where  $\bar{b}$  is a body force and it is assumed that the stress  $\sigma$  depends on only actual deformation. In linear elastic isotropic structures, the material tensor  $C$  is symmetric after a discrete process; therefore, the continuous displacement field  $u$  in  $\Omega_x$  is a unique solution. The schematic of topology optimization of a solid structure with specified field and boundary conditions is shown in Fig. 6. The principle of virtual displacements uses ensured satisfaction of equilibrium conditions within the weak form. The virtual work principle can be written as follows if virtual

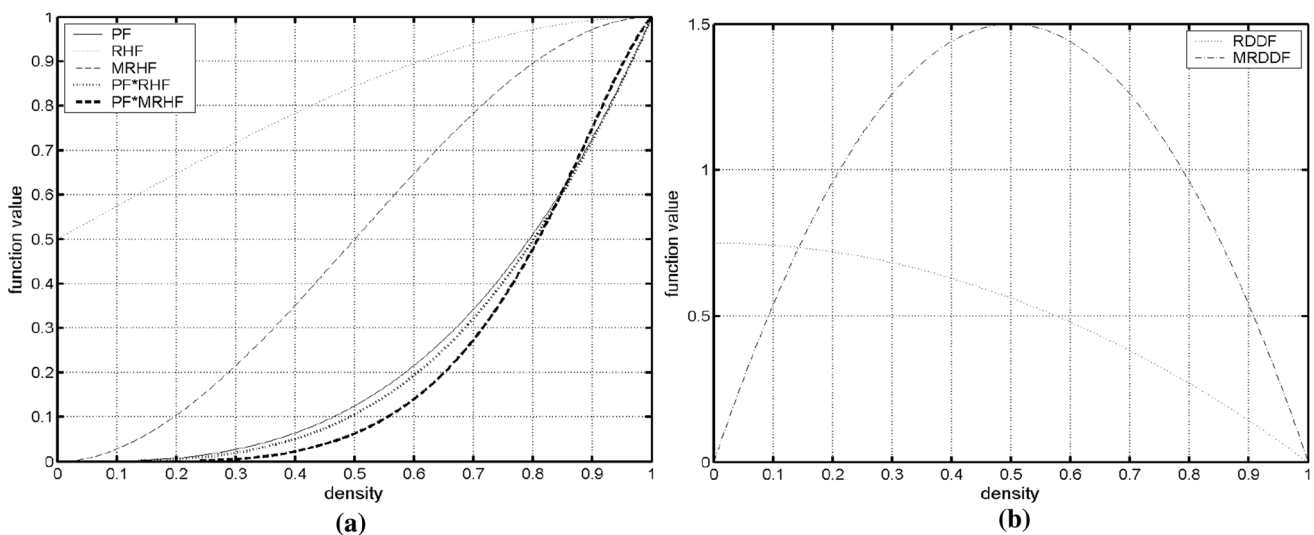


Fig. 5 Penalization relationships of SIMP: a penalization effect of MRHF b penalization effect of Dirac delta function

quantities  $\delta u$  and  $\delta \varepsilon$  are considered as variations (or differential) of the real quantities.

$$\delta \omega(\delta u, u, \Phi) = \delta \omega^i(\delta u, u, \Phi) + \delta \omega^a(\delta u, u) = 0; \delta u, u, \Phi \in V_u(\Omega_x) \subseteq H^1(\Omega_x) \tag{16}$$

where  $\delta \omega^i$  and  $\delta \omega^a$  denote a virtual internal work and virtual external work, respectively.  $\Phi$  is a property of material densities. The virtual internal work  $\delta \omega^i$  is expressed by virtual strain  $\delta \varepsilon$ , stress  $\sigma$  and a free-selectedly moved and regularized Heaviside function MRHF depending on the material density as follows:

$$\delta \omega^i = \int_{\Omega_x} \delta \varepsilon^T \sigma \text{MRHF}(\Phi) d\Omega_x \tag{17}$$

where it is assumed that the material density is independent of external forces, i.e., body and traction forces. The traction forces are conservative (or independent of displacement fields). Therefore, without the expression of a free-selected Heaviside function, the virtual external work  $\delta \omega^a$  is given by body force  $\bar{b}$ , traction force  $\bar{t}$  and virtual displacement field  $\delta u$  as follows:

$$\delta \omega^a = - \int_{\Omega_x} \delta u^T \bar{b} d\Omega_x - \int_{\Gamma_t} \delta u^T \bar{t} d\Gamma_t \tag{18}$$

Using Eq. (17) and (18), the equilibrium conditions of Eq. (16) are rewritten as:

$$\int_{\Omega_x} \delta \varepsilon^T \sigma \text{MRHF}(\Phi) d\Omega_x = \int_{\Omega_x} \delta u^T \bar{b} d\Omega_x + \int_{\Gamma_t} \delta u^T \bar{t} d\Gamma_t \tag{19}$$

Equation (16) means that for equilibrium to be ensured the total potential energy must be stationary for variations

of admissible displacements. It can be shown that in stable elastic situations the total potential energy is not only stationary but is a minimum. The weak form of the equilibrium can be differentiated by the principle of minimum potential energy.

$$\text{Minimize } \prod(u, \Phi) \rightarrow \delta \prod(u, \Phi) = 0; \delta u, u, \Phi \in V_u(\Omega_x) \subseteq H^1(\Omega_x) \tag{20}$$

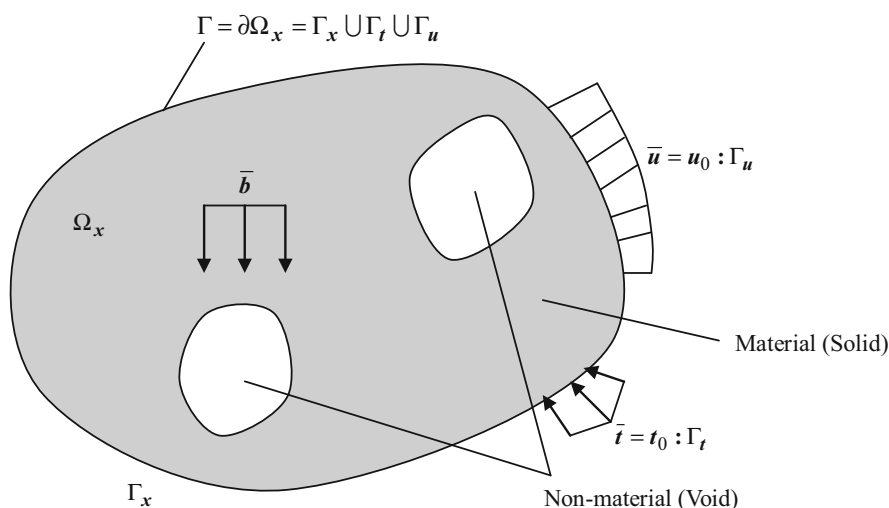
We note that by the principle of minimum potential energy, the objective function can be written as:

$$\begin{aligned} \prod(u, \Phi) &= \prod^i(u, \Phi) + \prod^a(u, \Phi) \\ &= \frac{1}{2} \int_{\Omega_x} \delta \varepsilon^T C \varepsilon \text{MRHF}(\Phi) d\Omega_x - \int_{\Omega_x} \delta u^T \bar{b} d\Omega_x \\ &\quad - \int_{\Gamma_t} \delta u^T \bar{t} d\Gamma_t \\ &= -\frac{1}{2} \int_{\Omega_x} \delta \varepsilon^T C \varepsilon \text{MRHF}(\Phi) d\Omega_x \end{aligned} \tag{21}$$

Here, according to discretization, the continuous material tensor  $C$  becomes dependent on the density–stiffness relationship of typical SIMP approach. The discontinuous Heaviside function is regularized as a smoothed and continuous form. For this purpose, the continuous objective function of Eq. (21) can be defined as Eq. (10) by discrete form. The inequality optimization condition is  $0 \leq \Phi \leq 1$  and an equality constraint describes the limit on the required amount of materials in terms of the constant volume  $V_0$  of design domain as follows:

$$\int_{\Omega_x} d\Omega_x - V_0 = 0 \tag{22}$$

**Fig. 6** The schematic for topology optimization of structure with specified field and boundary conditions



The general problem of structural topology optimization is specified as the objective function and constraints. The objective function is expressed as Eq. (21), and constraint conditions are the linear elastic equilibrium of Eq. (22) written in a weak form satisfying field and boundary conditions and volume constraint.

### 4 Analytical Sensitivity Method of Variational Approach

In general, the sensitivity of optimization problems such as objective functions or constraints can be calculated by analytical or numerical method (Lee et al. 2007). Since sensitivity errors of numerical sensitivity method may become great, the method is often used for verification of solutions. Analytical method is usually proper for the sensitivity of optimization problem due to small error of solution. The analytical sensitivity method is distributed as a discrete and a variational approach. In the discrete approach, optimization problems are at first discretized and then derivative is carried out. However, the variational approach firstly differentiates continuous optimization problems and secondly the derivative is discretized. Both approaches of analytical method can be solved by direct or adjoint method. Direct derivative of displacement field  $\nabla_s u$  is executed in the direct method; however, in the adjoint method using Lagrangian multiplier, the calculation of  $\nabla_s u$  it is not needed. The various methods for sensitivity analyses are shown in Fig. 7. The analytical sensitivity method of variational approach is utilized here, since the variational method is numerically more efficient than discrete method in certain optimization problems.

Since continuous displacement fields depend on design variables  $s$  (for instance, material densities), the total differential form of the objective function consists of parts of an explicit partial derivative and an implicit partial derivative, and it is defined as being introduced by Haug et al. (1986).

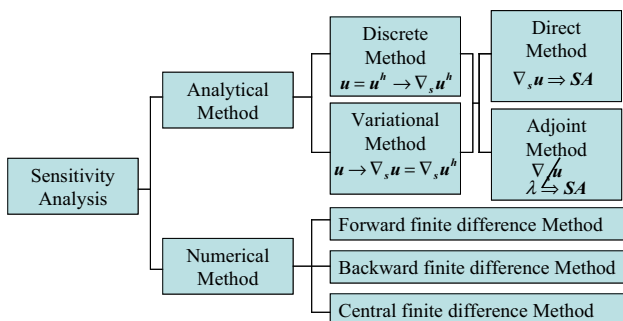


Fig. 7 Method of sensitivity analysis

$$\nabla_s f = \nabla_s^{ex} f + \overline{\nabla}_u f^T \nabla_s u \tag{23}$$

The total partial derivative is written as

$$\begin{aligned} \nabla_s f = & \frac{1}{2} \int_{\Omega_x} \varepsilon^T \nabla_s C(\Phi) \varepsilon \text{MRHF}(\Phi) d\Omega_x + \frac{1}{2} \\ & \int_{\Omega_x} \varepsilon^T C(\Phi) \varepsilon \text{MRDDF}(\Phi) d\Omega_x \quad : \text{explicit derivative} \\ & + \frac{1}{2} \int_{\Omega_x} \varepsilon^T C(\Phi) \nabla_u \varepsilon \text{MRHF}(\Phi) \nabla_s u d\Omega_x \quad : \text{implicit derivative} \end{aligned} \tag{24}$$

where MRDDF is a moved and regularized Dirac delta function and denotes derivative of MRHF. Through derivative of Eq. (19) satisfying field and boundary conditions, the terms of derivative of continuous displacement fields  $\nabla_s u$  by design variables can be written as

$$\begin{aligned} & \int_{\Omega_x} \delta u^T L^T C(\Phi) L \text{MRHF}(\Phi) \nabla_s u d\Omega_x \\ & = \int_{\Omega_x} \delta u^T \nabla_s \bar{b} d\Omega_x + \int_{\Gamma_t} \delta u^T \nabla_s \bar{t} d\Gamma_t \\ & - \int_{\Omega_x} \delta u^T \nabla_s L^T C(\Phi) L u \text{MRHF}(\Phi) d\Omega_x \\ & - \int_{\Omega_x} \delta u^T L^T \nabla_s C(\Phi) L u \text{MRHF}(\Phi) d\Omega_x \\ & - \int_{\Omega_x} \delta u^T L^T C(\Phi) \nabla_s L u \text{MRHF}(\Phi) d\Omega_x \\ & - \int_{\Omega_x} \delta u^T L^T C(\Phi) L u \text{MRDDF}(\Phi) d\Omega_x \end{aligned} \tag{25}$$

In order to calculate derivative of continuous displacement fields  $\nabla_s u$ , an adjoint method is used here. The adjoint method does not have to directly calculate continuous displacement fields with great numerical consumption. It is defined as

$$\bar{f} = f - \lambda \left[ \int_{\Omega_x} \delta \varepsilon^T \sigma \text{MRHF}(\Phi) d\Omega_x - \int_{\Omega_x} \delta u^T \bar{b} d\Omega_x - \int_{\Gamma_t} \delta u^T \bar{t} d\Gamma_t \right] \tag{26}$$

where the renewed objective function  $\bar{f}$  has an additional 0-term of static equilibrium, which is multiplied with a Lagrangian multiplier  $\lambda$ . The derivative of the Lagrangian multiplier  $\lambda$  disappears because of the 0-term. Therefore, the derivative of Eq. (26) is written as:

Lagrangian multipliers  $\lambda$  have arbitrary values. A specific Lagrangian multiplier value can be determined in Eq. (27) in order to remove the derivative of continuous displacement

$$\begin{aligned}
\nabla_s \bar{f} &= \nabla_s^{ex} f + \bar{\nabla}_u f^T \nabla_s u - \lambda \int_{\Omega_x} \delta u^T L^T C(\Phi) LMRHF(\Phi) \nabla_s u d\Omega_x \\
&\quad \text{---(a)=0} \\
&- \lambda \int_{\Omega_x} \delta u^T \nabla_s L^T C(\Phi) LuMRHF(\Phi) d\Omega_x - \lambda \int_{\Omega_x} \delta u^T L^T \nabla_s C(\Phi) LuMRHF(\Phi) d\Omega_x \\
&- \lambda \int_{\Omega_x} \delta u^T L^T C(\Phi) \nabla_s LuMRHF(\Phi) d\Omega_x - \lambda \int_{\Omega_x} \delta u^T L^T C(\Phi) LuMRDDF(\Phi) d\Omega_x \\
&+ \lambda \int_{\Omega_x} \delta u^T \nabla_s \bar{b} d\Omega_x + \lambda \int_{\Gamma_t} \delta u^T \nabla_s \bar{t} d\Gamma_t
\end{aligned} \tag{27}$$

fields which is numerically very expensive. Therefore, a specific equation (a) = 0 in Eq. (27) is made to include the specific Lagrangian multiplier value. After discretization of continuous design domain, the specific equation with a satisfied Lagrangian multiplier is expressed as

$$\begin{aligned}
&\hat{u}^T \int_{\Omega_\xi} B^T CB|J|MRHF(\Phi) d\Omega_\xi \nabla_s \hat{u} \\
&- \lambda \delta \hat{u}^T \int_{\Omega_\xi} B^T CB|J|MRHF(\Phi) d\Omega_\xi \nabla_s \hat{u} \\
&= 0
\end{aligned} \tag{28}$$

Through Eq. (28), the required Lagrangian multiplier value is written as follows:

$$\lambda = \hat{u}^T (\delta \hat{u}^T)^{-1} \tag{29}$$

Through Eqs. (28) and (29), a total partial derivative of the objective function in terms of design variable is finally expressed in discrete design domain as follows:

Under the assumptions that body force  $\bar{b}$ , traction force  $\bar{t}$ , differential matrix  $L$  and Jacobi matrix  $J$  are independent

of design variables, the total partial derivative of the objective function can be simply rewritten as follows:

$$\begin{aligned}
\nabla_s \bar{f} &= -\frac{1}{2} \hat{u}^T \int_{\Omega_\xi} B^T \nabla_s C(\Phi) B|J|MRHF(\Phi) d\Omega_\xi \hat{u} \\
&- \frac{1}{2} \hat{u}^T \int_{\Omega_\xi} B^T CB|J|MRDDF(\Phi) d\Omega_\xi \hat{u}
\end{aligned} \tag{31}$$

## 5 Numerical Examples and Discussions

### 5.1 Topology Optimization of 2D Cantilever Beam Structures

As the first numerical examples, elastostatic cantilever beams as shown in Fig. 8 are considered to evaluate the proposed method. Figure 8a, b are structures of length of 4.8 m and height of 4.0 m and are discretized as design domain of  $48 \times 40$  finite elements with 4-node. Suppose the design domain is made of regular square grid.

$$\begin{aligned}
\nabla_s \bar{f} &= \frac{1}{2} \hat{u}^T \int_{\Omega_\xi} B^T \nabla_s C(\Phi) B|J|MRHF(\Phi) d\Omega_\xi \hat{u} + \frac{1}{2} \hat{u}^T \int_{\Omega_\xi} B^T C(\Phi) B|J|MRDDF(\Phi) d\Omega_\xi \hat{u} \\
&- \hat{u}^T \left[ \int_{\Omega_\xi} \nabla_s B^T C(\Phi) B|J|MRHF(\Phi) d\Omega_\xi \hat{u} + \int_{\Omega_\xi} B^T \nabla_s C(\Phi) B|J|MRHF(\Phi) d\Omega_\xi \hat{u} + \int_{\Omega_\xi} B^T C(\Phi) \nabla_s B|J|MRHF(\Phi) d\Omega_\xi \hat{u} \right. \\
&\quad \left. + \int_{\Omega_\xi} B^T C(\Phi) B|J|\bar{\delta}(\Phi) d\Omega_\xi \hat{u} - \int_{\Omega_\xi} N^T \nabla_s \bar{b}|J| d\Omega_\xi - \int_{\Omega_\eta} N^T \nabla_s \bar{t} \sqrt{|G_e|} d\Omega_\eta \right]
\end{aligned} \tag{30}$$



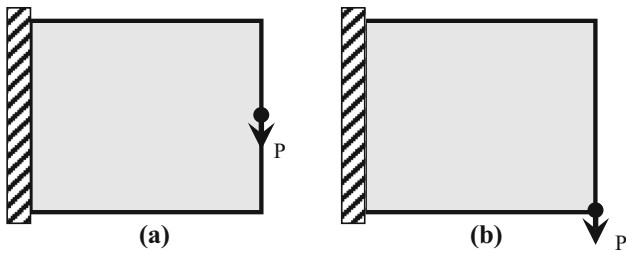


Fig. 8 Problem statements of 2D cantilever beams

A concentrated load  $P = -360N$  at the right side of structure is applied. The material parameters are Young's module  $E = 2.1 \times 10^6 \text{ kg/cm}^2$  and Poisson's ratio  $\nu = 0.3$ . Plane stress is assumed in 2D. The penalty parameter  $k = 3.0$  and updated material density  $0 \leq \Phi_i \leq 1$  are chosen for SIMP method. The initial values of density variables are set to be  $\Phi_0 = 0.3$  onto all finite elements. For filter method, the filter exponent  $\beta = 3.0$  and the radius  $r = 1.5$ . The filter method was utilized for all numerical examples.

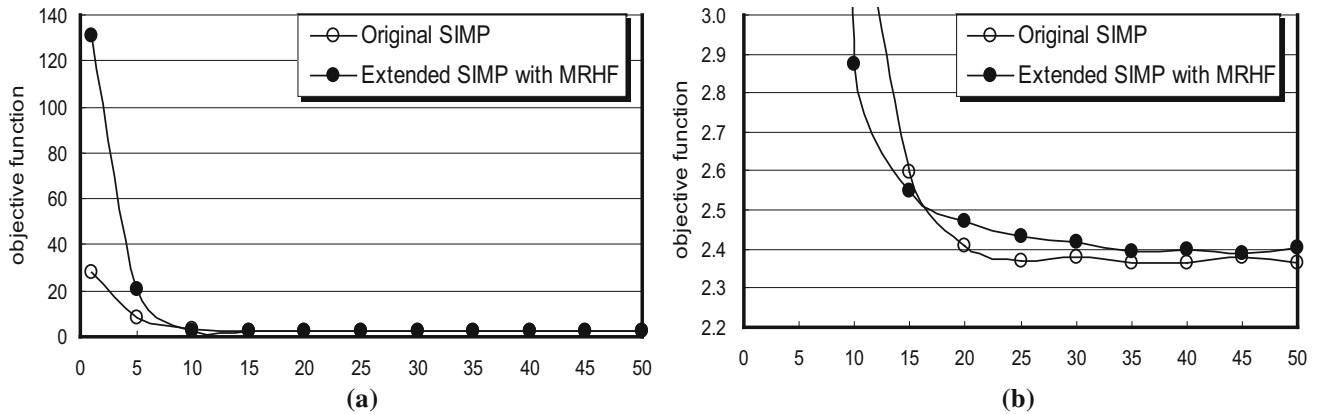


Fig. 9 History of optimization convergence a iteration (large scale) b iteration (small scale)

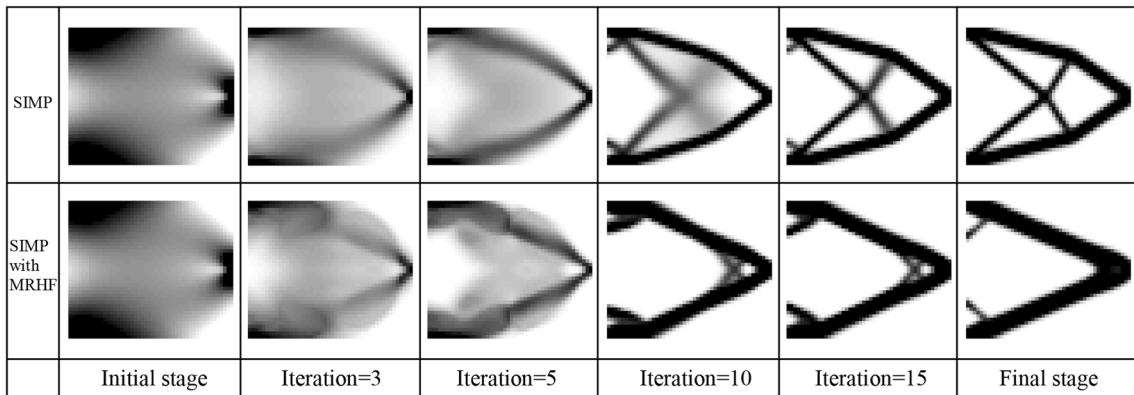


Fig. 10 Material density distribution in optimization iterations

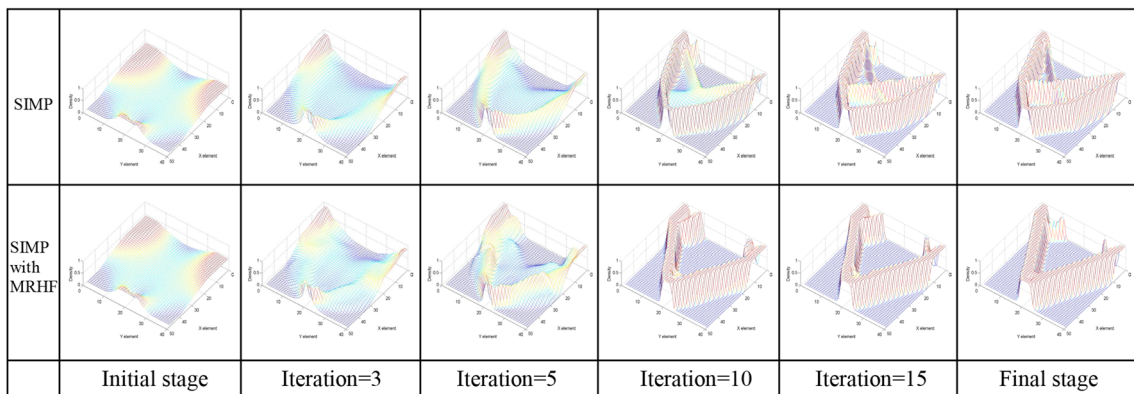


Fig. 11 3D density function in optimization iterations

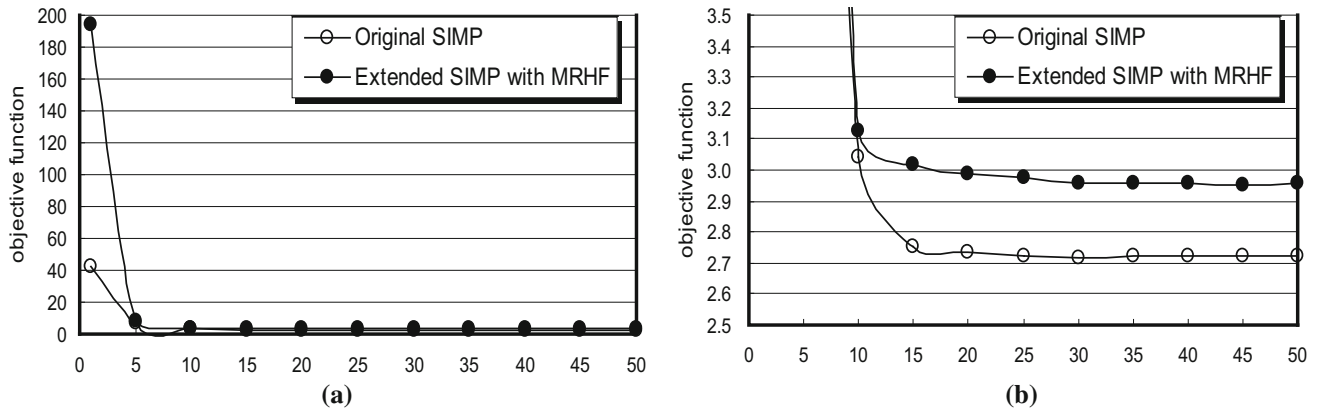


Fig. 12 History of optimization convergence **a** iteration (large scale) **b** iteration (small scale)

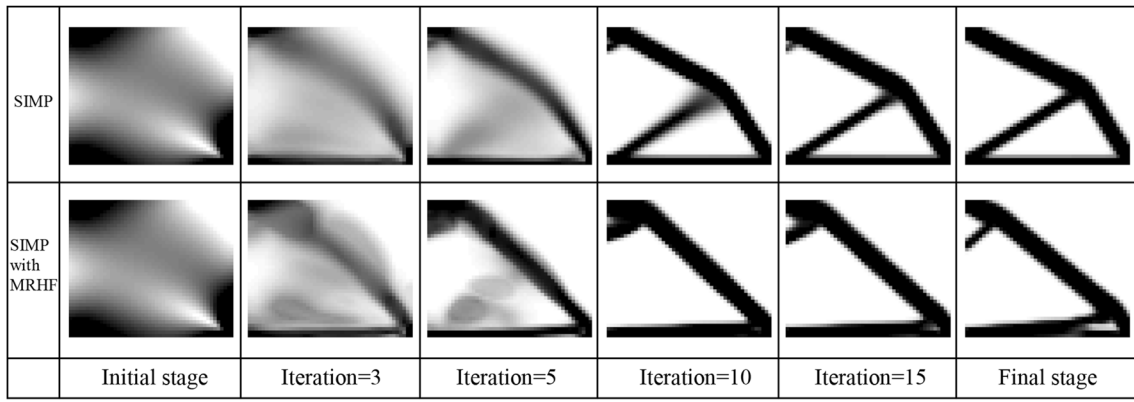


Fig. 13 Material density distribution in optimization iterations

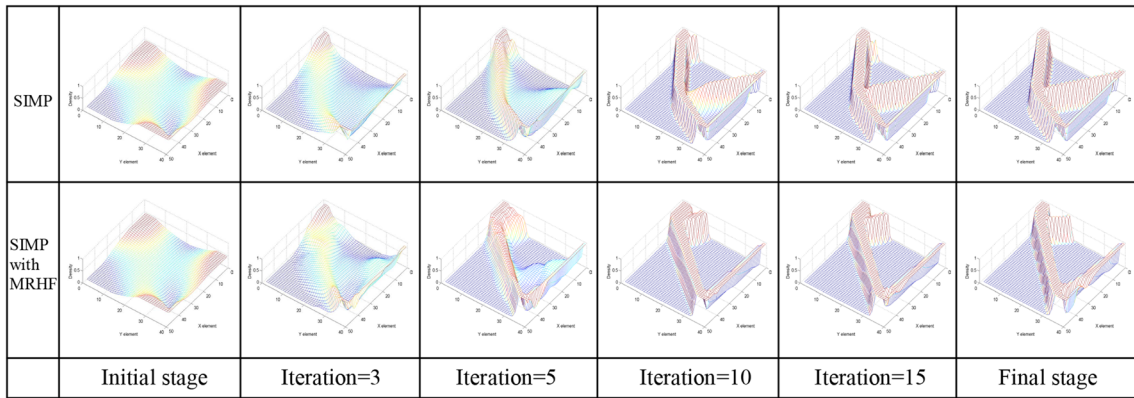


Fig. 14 3D density function in optimization iterations

Here, objective function is defined as a minimal strain energy (N·m) or a maximal stiffness and 30% constraint volume of total volumes is used as optimization constraint. In this example, MRHF of Eq. (6) is implemented for the penalization of SIMP approach.

Figure 9 shows histories of convergence in both cases of original SIMP and extended SIMP with MRHF in Fig. 8a. The histories start with great differences at initial

optimization stage, and then, these take similar convergences at final stage. The iteration results of Fig. 9 are visually described as changing material density distributions as shown in Fig. 10. Figure 11 shows visual changes of 3D density functions of optimization iterations. It can be found that although both methods take similar convergence behaviors, different optimal topologies are obtained.

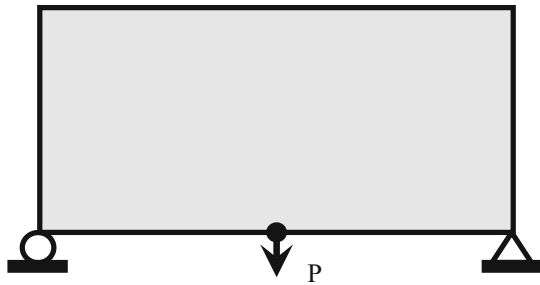


Fig. 15 Problem statements of 2D Michell beam structure

The histories of convergence of SIMP and SIMP using MRHF about the cantilever beam of Fig. 8b is shown in Fig. 12.

The material density distribution and 3D density function of their visual iterations are, respectively, illustrated in Figs. 13 and 14. It can be seen from the results that the convergences of objective function and optimal solutions of shapes and topologies are different in SIMP and SIMP using MRHF and these situations are similar to those of Fig. 8a.

### 5.2 Topology Optimization of 2D Michell Beam Structure

The second example is a 2D Michell beam structure as shown in Fig. 15. All applied design conditions are identified with those of example 5.1. The roller and hinge are supported at the bottom corner of right and left sides, respectively. At the bottom center, a concentrated load is applied. Here,  $60 \times 30$  square finite elements with 4-node are used for discretization of design domain  $6 \text{ m} \times 3 \text{ m}$ .

Figure 16 is shown in convergent histories of objective function in cases of original SIMP and SIMP using MRHF, and their iteration results are illustrated in Figs. 17 and 18. The convergent value of SIMP using MRHF is a little worse than that of original SIMP and convergent values almost identify each other. Nevertheless, both methods are considerably different with respect to optimal topologies.

### 5.3 Topology Optimization of 2D Double-Clamped Beam Structure

The third example is a double-clamped beam with a vertically concentrated load at the center of structure as shown

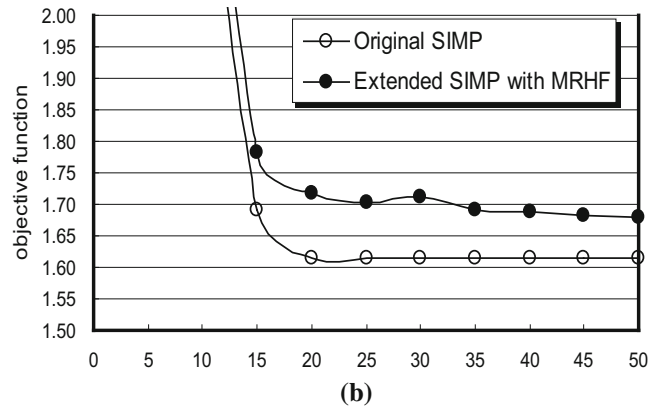
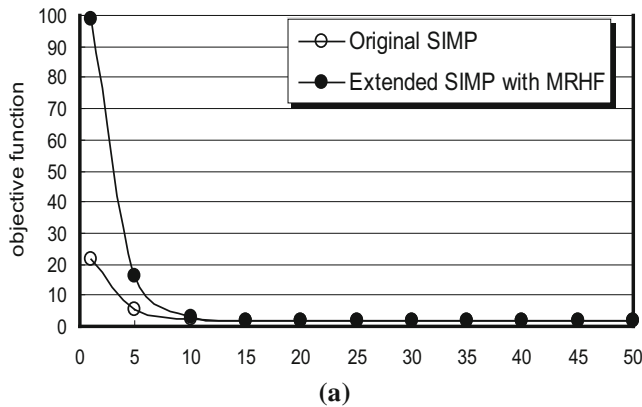


Fig. 16 History of optimization convergence **a** iteration a (large scale) **b** iteration (small scale)

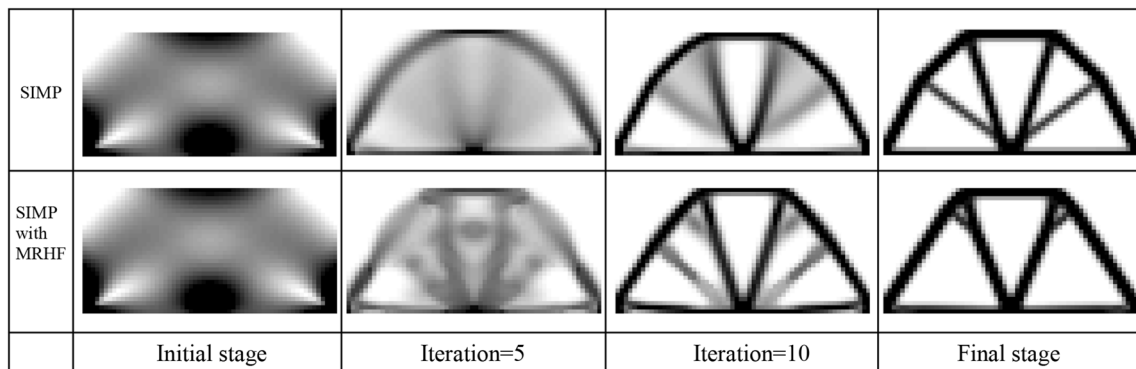


Fig. 17 Material density distribution in optimization iterations

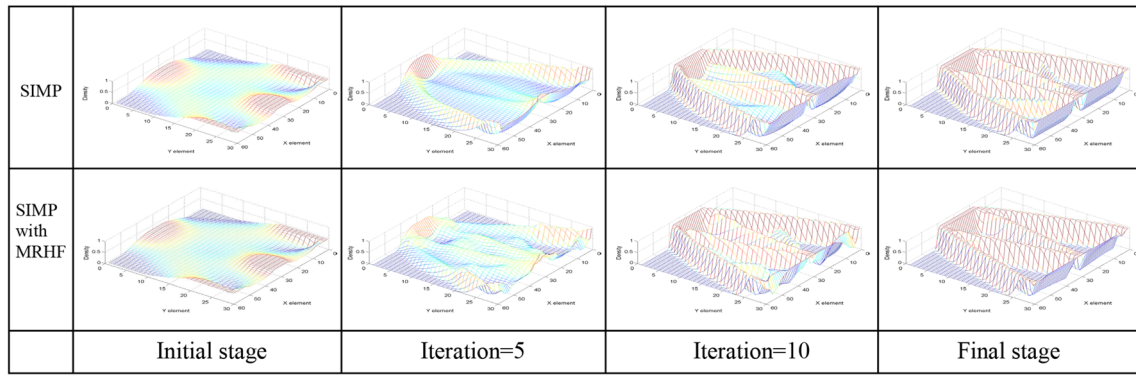


Fig. 18 3D density function in optimization iterations

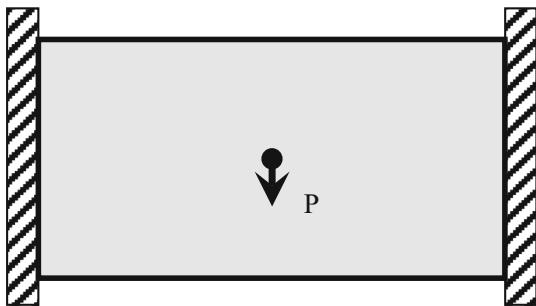


Fig. 19 Problem statements of 2D double-clamped beam structure

in Fig. 19. All design conditions for topology optimization and discretization of  $60 \times 30$  are equal to example 5.2.

The convergent histories of objective function in original SIMP and SIMP using MRHF are described in Fig. 20. During iterations, weak oscillations of convergent curves occur at convergent curves in both methods.

Their visual results are shown in Figs. 21 and 22. It can be found that optimal topologies of both methods almost match and the result is different compared with those of example 5.1 and 5.2.

### 5.4 Penalization Effects of MRHF: Clear Contours of Density Distribution and Free-Checkerboards

The checkerboard-like pattern of original SIMP approach observed previously in the Sect. 3 can be removed or reduced by various methods, for example the work by Bendsøe and Soares (1993), Kumar and Gossard (1996), Byun et al. (2004) in structural engineering. However, in this study, we consider a penalization by MRHF in addition to the original penalty function in typical SIMP. Therefore, in order to remove the checkerboard pattern, a penalization process is followed with MRHF term which is multiplied with penalty function of typical SIMP.

When all examples are considered, Fig. 23 shows optimal material density distributions of original SIMP and SIMP with MRHF without the use of filter method, which has been implemented for the removal of checkerboard phenomena. It can be seen from Fig. 23 that the penalization of SIMP using MRHF reduces checkerboards. It seems that the effect is similar to the results of filter method in Sects. 5.1–5.3. Note that clear boundaries of 0–1 without gray scales in material density distributions can be obtained through this penalization of SIMP using MRHF,

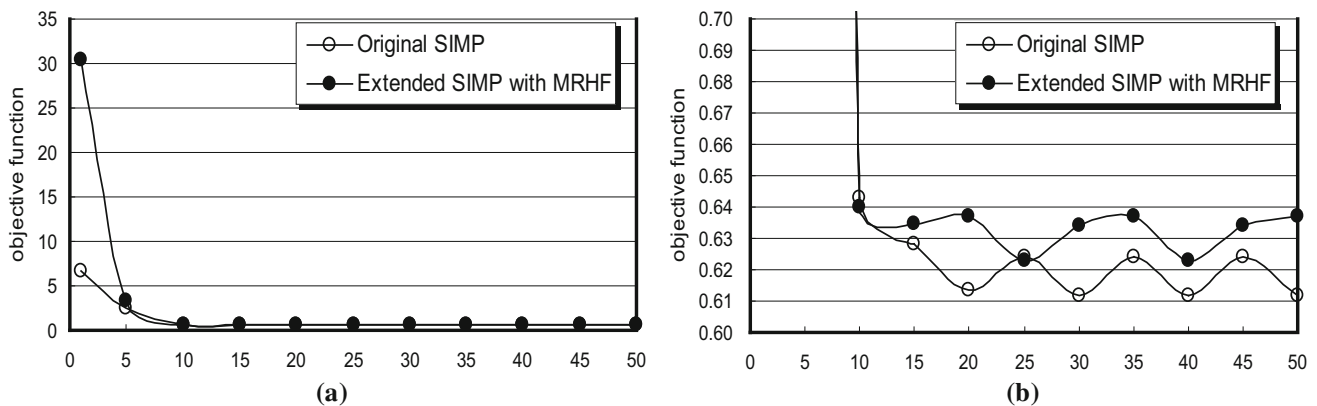
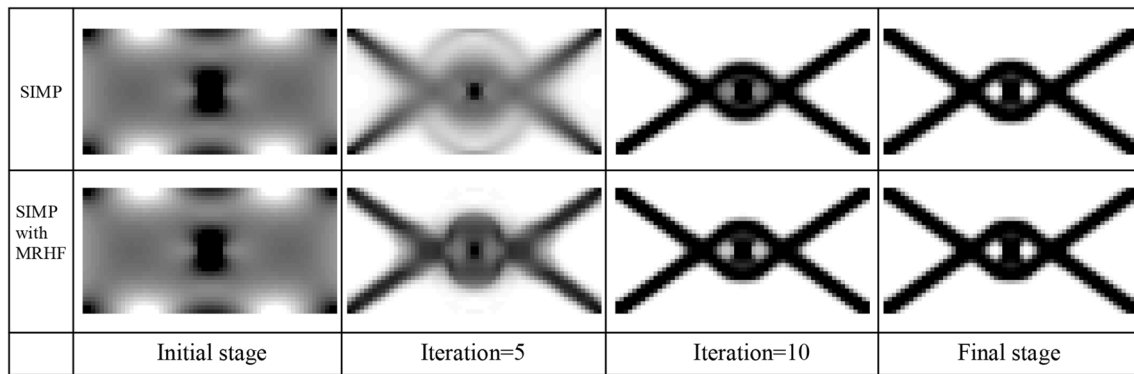
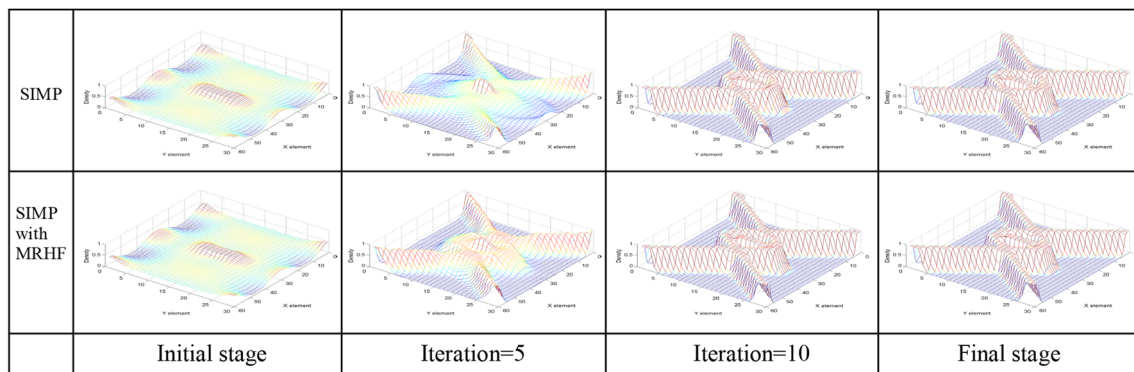


Fig. 20 History of optimization convergence a (large scale) b iteration (small scale)



**Fig. 21** Material density distribution in optimization iterations



**Fig. 22** 3D density function in optimization iterations

while optimal solutions by the penalization of SIMP with filter method are smoothed but unclear as shown in Figs. 10, 13, 17 and 21.

Table 1 illustrates 2–3 times savings of computational time in case of SIMP using MRHF without the filter method, compared with the use of filter method of typical SIMP. Table 2 shows optimal results of original SIMP and SIMP using MRHF and filter method. It can be even seen that computational time of the proposed SIMP using MRHF is similar to that of original SIMP.

The proposed approach has one similarity compared with a method presented in Belytschko et al. (2003). It uses implicit functions as design variables to describe topology of structures. The similarity is that both methods regularize Heaviside function to archive 0–1 solutions with numerical stability. However, the method employed by Belytschko et al. uses implicit function to describe topology of structures and is implemented by nodal values of design variable to project those values onto the element domain. It requires many numbers of design variables and its convergence rate may be very slow. Here, the proposed method seeks improved solutions in the range of the conventional SIMP formulation as an element density-based design.

## 6 Conclusions

In this paper, an improved SIMP approach based on the regularization was proposed for material topology optimization of linear elastostatic structures. The key point of this study is to utilize a moved and regularized Heaviside function into the penalty formulation of SIMP approach. The proposed penalization saves computational times for free-checkerboard patterns, since no filter method is needed in optimization procedures. Moreover, clear boundaries between material and no material phases are yielded as optimal solutions in design domain. Various regularization processes of Heaviside function which have been introduced in other research literature can be implemented in MRHF as mentioned in Eqs. (6)–(9) and are also suitable for the present approach.

Their application to numerical examples successfully reduced checkerboard patterns without the use of filter method, and, in addition, even produced obvious boundaries of optimal solution under appropriate convergences of optimization. Although this method of representing the new penalization relations of Young's modulus and density was stimulated by the devised MRHF and original SIMP approach for topology optimization design, it is expected

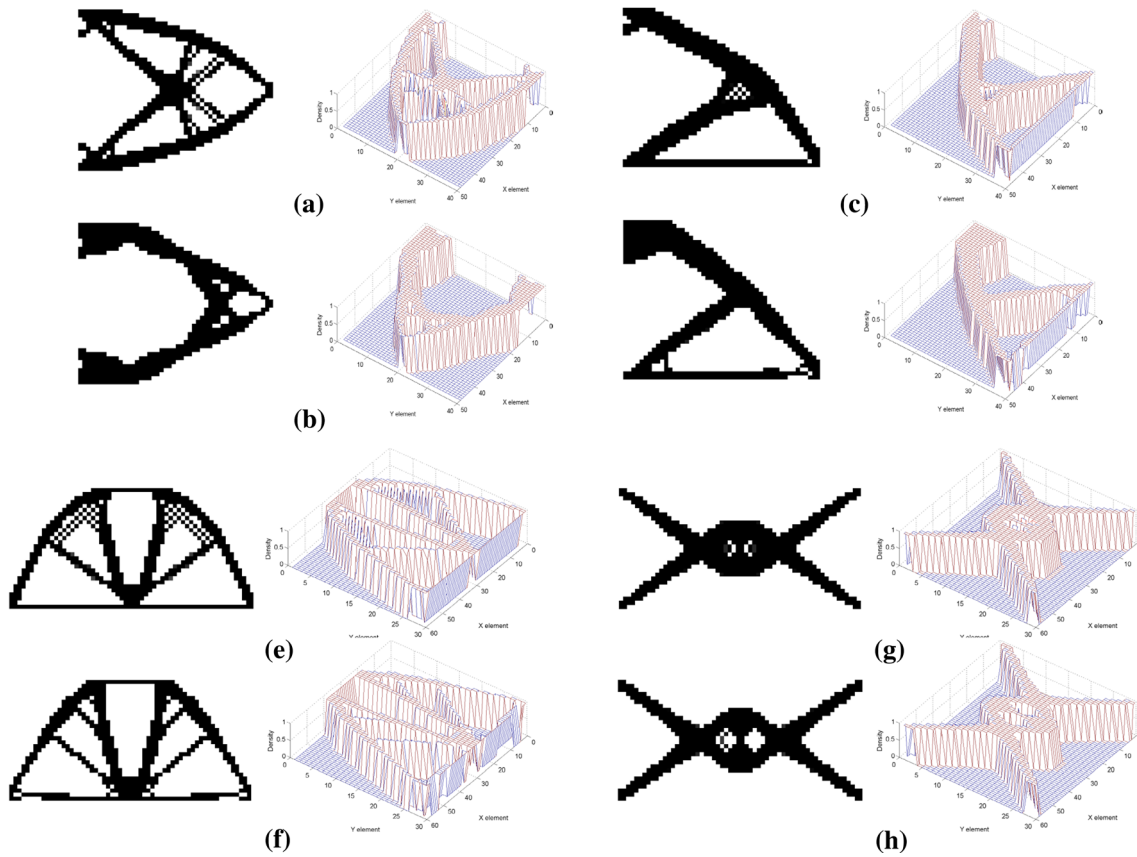


Fig. 23 Comparisons of optimal solutions: **a, c, e, g** original SIMP without filter method **b, d, f, h** SIMP with MRHF and without filter method

**Table 1** Optimal results by original SIMP with filter method (FM) and SIMP using MRHF without filter method (FM)

Type of problem	Cantilever of Fig. 8a		Cantilever of Fig. 8b		Michell beam		Double-clamped beam	
	Original SIMP + FM	SIMP + MRHF	Original SIMP + FM	SIMP + RHF	Original SIMP + FM	SIMP + MRHF	Original SIMP + FM	SIMP + MRHF
Number of FE	1920		1920		1800		1800	
Objective function (N·m)	2.3644	3.1149	2.7252	3.2446	1.6142	1.6743	0.6120	0.5475
Computational time (s)	801.1090	342.9540	866.2180	334.5000	776.7660	279.4060	480.7660	265.9530

**Table 2** Optimal results by original SIMP and SIMP using MRHF and filter method (FM)

Type of problem	Cantilever of Fig. 8a		Cantilever of Fig. 8b		Michell beam		Double-clamped beam	
	Original SIMP	SIMP + MRHF + FM	Original SIMP	SIMP + MRHF + FM	Original SIMP	SIMP + MRHF + FM	Original SIMP	SIMP + MRHF + FM
Number of FE	1920		1920		1800		1800	
Objective function (N·m)	2.4262	2.4021	2.7487	2.9602	1.4873	1.6785	0.5752	0.6372
Computational time (s)	348.9690	672.1570	328.4220	850.5780	329.4060	804.7500	270.9220	913.9850

that there will be other applications for this effect in various analyses and design problems.

**Acknowledgements** This research was supported by a grant (code# NRF-2017R1D1A1B03031350) from the National Research Foundation of Korea (NRF) funded by the Korea government.

## References

- Belytschko T, Xiao SP, Parimi C (2003) Topology optimization with implicit functions and regularization. *Int J Numer Meth Eng* 57:1177–1196
- Bendsøe MP (1989) Optimal shape design as a material distribution problem. *Struct Optim* 1:193–202
- Bendsøe MP, Haber R (1993) The Michell layout problem as a low volume fraction limit of the homogenization method for topology design: an asymptotic study. *Struct Optim* 6:263–267
- Bendsøe MP, Kikuchi N (1988) Generating optimal topologies in structural design using a homogenization method. *Comput Methods Appl Mech Eng* 71:197–224
- Bendsøe MP, Sigmund O (1999) Material interpolations in topology optimization. *Arch Appl Mech* 69:635–654
- Bendsøe MP, Soares CAM (1993) *Topology design of structures*. Kluwer, Norwell
- Bourdin B (2001) Filters in topology optimization. *Int J Numer Meth Eng* 50:2143–2158
- Byun JK, Lee JH, Park IH (2004) Node-based distribution of material properties for topology optimization of electromagnetic devices. *IEEE Trans Magn* 40:1212–1215
- Cheng G, Olhoff N (1981) An investigation concerning optimal design of solid elastic plates. *Int J Solids Struct* 17(3):305–323
- Diaz AR, Bendsøe MP (1992) Shape optimization of structures for multiple loading conditions using a homogenization method. *Struct Optim* 4:17–22
- Diaz RI, Sigmund O (1995) Checkerboards patterns in layout optimization. *Struct Optim* 10:40–45
- Fujii D, Chen BC, Kikuchi N (2001) Composite material design of two-dimensional structures using the homogenization design method. *Int J Numer Meth Eng* 50:2031–2051
- Guest JK, Prevost JH, Belytschko T (2004) Achieving minimum length scale in topology optimization using nodal design variables and projection function. *Int J Numer Meth Eng* 61:238–254
- Haftka RT, Guerdal Z (1992) *Elements of structural optimization—third revised and expanded edition*. Kluwer Academic Publishers, Dordrecht
- Haug EJ, Choi KK, Komkov V (1986) *Design sensitivity analysis of structural systems*. Academic Press, Orlando
- Kumar AV, Gossard DC (1996) Synthesis of optimal shape and topology of structures. *J Mech Des* 118:68–74
- Lee DK, Shin SM (2007) Numerical aspects of element- and nodal-based material topology optimization of structures. *J Solid Mech Mater Eng* 1(5):656–666
- Lee DK, Shin SM (2015) Optimizing structural topology patterns using regularization of Heaviside function. *Struct Eng Mech* 55(6):1157–1176
- Pahlevani Z, Ebrahimi R (2013) Optimization of specific die profiles in thin walled tube extrusion. *IJST, Trans Mech Eng* 37(M2):203–215
- Sigmund O (2001) A 99 topology optimization code written in Matlab. *Struct Multidiscip Optim* 21:120–127
- Sigmund O, Petersson J (1998) Numerical instabilities in topology optimization: a survey on procedures dealing with checkerboards, mesh-dependencies and local minima. *Struct Optim* 16(1):68–75
- Zienkiewicz OC, Campbell JS (1973) Shape optimization and sequential linear programming. In: Gallagher RH, Zienkiewicz OC (eds) *Optimum structural design*. Wiley, Hoboken, pp 109–126